Generating Quantitative pH Maps in Hyper-acute Stroke Patients Using Amide Proton Transfer (APT) Imaging

Yee Kai Tee[1], George Harston[2], Nicholas Blockley[3], Thomas Okell[3], Jacob Levman[1], Martino Cellerini[4], Fintan Sheerin[4], Peter Jezzard[3], James Kennedy[2], Stephen Payne[1], and Michael Chappell[1]

[1]*Department of Engineering Science, Institute of Biomedical Engineering, University of Oxford, Oxford, Oxfordshire, United Kingdom,* [2]*Acute Stroke Programme, Radcliffe Department of Medicine, University of Oxford, Oxfordshire, United Kingdom,* [3]*FMRIB, Nuffield Department of Clinical Neurosciences, University of Oxford, Oxfordshire, United Kingdom,* [4]*Department of Neuroradiology, Oxford University Hospitals NHS Trust, Oxfordshire, United Kingdom*

Target Audience: Clinicians and researchers who are interested in measuring pH using amide proton transfer (APT) imaging for hyper-acute stroke diagnosis.

Purpose: APT imaging is a pH-weighted imaging method based on chemical exchange saturation transfer (CEST) that has potential to identify salvageable tissue better than the current clinical practice after ischemic stroke [1]. Despite the potential of APT imaging to measure pH, most of the literature thus far has focused on generating pH-weighted contrast rather than quantitative pH maps. In this study, a recently introduced quantitative Bayesian model-based analysis [2] was extended to produce quantitative pH maps using a previously calibrated relationship and applied to APT data acquired in healthy subjects and hyper-acute stroke patients.

Methods: 2 healthy volunteers and 6 patients presenting with hyper-acute stroke symptoms (< 6 hours of onset) were recruited and scanned using a 3T Siemens Verio scanner following informed consent or agreement from a representative according to a research protocol agreed by the UK NRES committee (ref: 12/SC/0292).

Diffusion weighted imaging (DWI) with 3 directions (b = 0 and 1000 s/mm^3), T_1 structural imaging, and single-slice transverse APT imaging as per Ref. [2] were performed; the APT plane was chosen by an attending clinician based on the lesion seen on the DWI scan with slice thickness = 5 mm. APT saturation was achieved using 50 Gaussian pulses of duration 20 ms with 20 ms spacing to achieve an equivalent continuous saturation B_1 value of 0.535 μT (average power). APT data were acquired for a range of saturation frequency offsets from -4.5 to 4.5 ppm and at ± 300 ppm, resulting in 32 APT images acquired in slightly less 3 mins.

Table 1: Model parameters with prior values – mean and standard deviation (SD) of a normal distribution, modified from [2]; $i \in \{w, APT, MT+NOE\}$.

Parameter	Water Pool		APT Pool		MT+NOE Pool	
	Mean	SD	Mean	SD	Mean	SD
M_0	0	10^6	-	-	-	-
M_0^i/M_0^w	-	-	0.09/112	0.02/112	0	0.01
$k_{i\,to\,w}$, (Hz)	-	-	20	-	30	-
$\log(k_{i\,to\,w})$	-	-	3.0	1.0	3.4	1.0
T_{1i}, (s)	1.3	0.15	0.77	0.15	1.0	0.15
T_{2i}, (ms)	70	14	10	2	0.2	0.04
ω_i, (ppm)	0	0.1	3.5	0.1	-2.41	0.1

FLIRT in the FSL package [3] was used to correct for the motion artefacts. A 3-pool model consisting of water (w), amide (APT) and magnetization transfer + nuclear overhauser effect (MT+NOE) was fitted voxelwise to the measured z-spectra using a Bayesian algorithm [2] with prior values of each parameter given in Table 1 and treating the pulsed saturation as its continuous approximation using average power [4]. The pure APT effect, APTR*, without spillover and MT+NOE contamination, was calculated using the fitted parameters from the model-based analysis to generate an ideal 2-pool, water plus amide, z-spectrum which was compared to an ideal 1-pool model of water: APTR* = $[M_{water}(3.5ppm) - M_{water+APT}(3.5ppm)]/M_0^w$ – Eqn. (1), where M_0^w is the fitted unsaturated water signal and $M(3.5\ ppm)$ refers to the simulated magnetization at 3.5 ppm using either the fitted parameters from water pool or both water and amide pools.

Previously, a relationship between amide proton exchange rate, $k_{APT\,to\,w}$, and intracellular pH was found to be (Fig.1a) [1]: $pH = 6.4 + \log_{10}[k_{APT\,to\,w}/5.57]$ – Eqn. (2). For the proposed model-based approach, an idealised APTR* vs pH relationship could also be formed using Eqn. 2 and simulations. By assuming water (M_0^w) and amide proton concentrations (M_0^{APT}) equal to 112M and 100mM [5], respectively, and the remaining parameters in the 2-pool model (water and APT) to have the mean values in Table 1, saturated by B_1 = 0.535 μT and saturation time = 2 s (to match the experiment), a range of idealised APTR* vs different pH values (by varying $k_{APT\,to\,w}$ in Eqn. (2)) could be simulated and a relationship between them could then be formed.

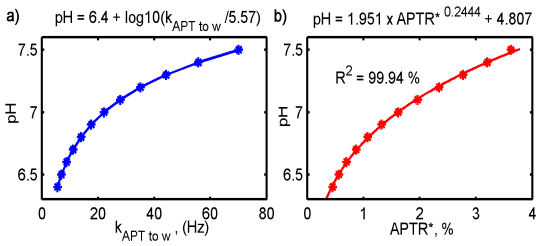

Fig.1: a) pH and amide proton exchange rate ($k_{APT\,to\,w}$) relationship from [1]; b) pH vs APTR relationship formed using the relationship in a) and simulations.*

For the measured APT data, an idealised APTR* could be calculated according to Eqn. (1) using only 3 parameters from the model fitting: 1) M_0^w; 2) $k_{APT\,to\,w}$; and 3) M_0^{APT}. Since the variations of the remaining parameters in the ideal 1- and 2-pool model should have been accounted for by the Bayesian fitting algorithm, they were assumed to have values from the simulations used to generate the idealised APTR* vs pH relationship so that the calculated APTR* could be converted to quantitative pH maps using the relationship formed based on Eqn. (2) and simulations.

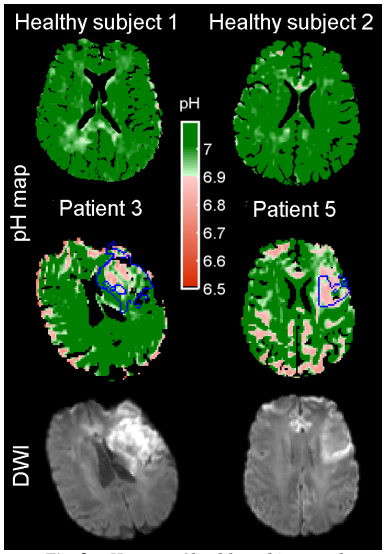

Fig. 2: pH maps of healthy subjects and representative patients generated using the relationship in Fig. 1b); DWI (b = 1000) of patients are plotted directly below their respective pH map.

Results: Fig. 1b) shows the pH vs APTR* relationship formed using simulations, where pH = 1.951 x APTR*$^{0.2444}$ + 4.807. When the relationship in Fig. 1b) was applied on the calculated idealised APTR* in healthy volunteers, relatively homogenous pH maps were obtained with tissue having pH values of 7.04 ± 0.07 as shown in Fig. 2. The pH colour bar was set according to [1], where 7.11 ± 0.13 is normal (green) and below 6.9 is ischemic (pink to red), which effectively thresholds the results. In patients, lower pH values were observed in the ischemic area, as identified by a clinician based on the DWI data (Fig. 2 – blue line area, pH = 6.92 ± 0.13). Outside the immediate vicinity of the ischemic tissue the majority of the tissue was within a normal range (green), consistent with the healthy subjects, although some areas of apparent low pH were observed particularly near regions of high CSF contamination.

Discussion: In this study, quantitative pH maps were demonstrated in healthy subjects and hyper-acute stroke patients using the relationship of pH and APTR* formed from a previously published calibration between pH and $k_{APT\,to\,w}$. These are the first quantitative pH maps generated from APT imaging in hyper-acute stroke patients to the best of our knowledge. Although realistic pH maps were generated, artefacts (low pH values) were seen in the non-ischemic tissue area too, especially in the patient cases. The concentration of amide protons was set to be 100mM in the simulations to generate the relationship in Fig. 1b. This is probably one of the main factors contributing to the artefacts seen on the generated pH maps, aside from motion artefacts, because of low amide proton concentration in non-tissue areas such as CSF. Partial volume of these regions with tissue would cause the model to estimate it as having a low APT effect. This issue has also been reported by others using magnetization transfer asymmetry analysis [6], suggesting that a post-processing partial volume correction technique may be required. Both $k_{APT\,to\,w}$ and M_0^{APT} were used here to calculate the idealised APTR* instead of using $k_{APT\,to\,w}$ alone, this is based on the observation that within a model-based analysis these 2 parameters are highly correlated and thus it is difficult to separate their effect [2]. However, it is generally assumed that in hyper-acute ischemia, amide proton concentration is approximately invariant from normal values [1]. Nevertheless, this assumption might not hold in other cases such as later imaging of stroke patients (> 24 hours) or in tumours.

References: 1. Zhou *et al.*, Nat. Med. 9:1085-1090, 2003. 2. Chappell *et al.*, MRM. 70(2):556-567, 2013. 3. Jenkinson *et al.*, NeuroImage, 17(2):825-841, 2002. 4. Tee *et al.*, JMR. 222:88-95, 2012. 5. Sun *et al.* MRM. 57(2):405-410, 2007. 6. Zhao *et al.*, MRM. 66(4):1033-1041, 2011.